Original Research Paper

Basal astrocyte and microglia activation in the central nervous system of Familial Hemiplegic Migraine Type I mice

Giulia Magni[1], Marta Boccazzi[1,], Antonella Bodini[2], Maria P Abbracchio[1], Arn MJM van den Maagdenberg[3], Stefania Ceruti[1*]

[1]Department of Pharmacological and Biomolecular Sciences (DiSFeB), Università degli Studi di Milano, Milan, Italy

[2]Institute for Applied Mathematics and Information Technologies "Enrico Magenes", National Research Council, Milan, Italy

[3]Departments of Neurology and Human Genetics, Leiden University Medical Centre, Leiden, Netherlands.

*Author for correspondence:

Dr. S. Ceruti, Department of Pharmacological and Biomolecular Sciences (DiSFeB), Università degli Studi di Milano, via Balzaretti 9, 20133 Milan, Italy; Tel. +39-0250318261; Fax +39-0250318284; Email: stefania.ceruti@unimi.it.

Abstract

Background

Gain-of-function missense mutations in the α_{1A} subunit of neuronal $Ca_V2.1$ channels, which define Familial Hemiplegic Migraine Type 1 (FHM1), result in enhanced cortical glutamatergic transmission and a higher susceptibility to cortical spreading depolarization. It is now well established that neurons signal to surrounding glial cells, namely astrocytes and microglia, in the central nervous system, which in turn become activated and in pathological conditions can sustain neuroinflammation. We and others previously demonstrated an increased activation of pro-algogenic pathways, paralleled by augmented macrophage infiltration, in the trigeminal ganglia of FHM1 mutant mice ex vivo and in vitro. Hence, we hypothesize that astrocyte and microglia activation may occur in parallel in the central nervous system.

Methods

We have evaluated signs of reactive glia in brains from naïve FHM1 mutant mice in comparison with wild type animals by immunohistochemistry and Western blotting.

Results

Here we show for the first time in the naïve FHM1 mutant mouse brain signs of reactive astrogliosis, and microglia activation.

Conclusions

Our data reinforce the involvement of glial cells in migraine, and suggest that modulating such activation may represent an innovative approach to reduce pathology.

Keywords

Reactive astrocytes, activated microglia, neuroinflammation, migraine

Introduction

Familial hemiplegic migraine (FHM) is a monogenic subtype of migraine with aura, characterized by recurrent attacks of headache that are accompanied by auras consisting of transient neurological symptoms that include visual, sensory, and motor disturbances [1]. Transgenic FHM1 mutant mice that express gain-of-function missense mutations in *CACNA1A*, which encodes the α_{1A} subunit of voltage-gated $Ca_V2.1$ calcium channels, revealed neuronal involvement with increased $Ca_V2.1$ channel function and enhanced cortical glutamatergic neurotransmission that can explain the increased susceptibility to experimentally induced cortical spreading depolarization (CSD) [2, 3]. The consequences of the mutation may, however, extend to cell types that surround neurons in the brain. For instance, there is evidence suggesting that neuronal hyperexcitability can trigger so-called "neurogenic neuroinflammation", which involves the vascular and glial cell components of brain tissue, and can recruit immune cells from the bloodstream [4]. Although an homeostatic role for neuroinflammation has been postulated, it might also lead to further release of pro-inflammatory mediators by surrounding activated glial cells, namely reactive astrocytes and microglia, which in turn may trigger or aggravate an underlying pathological condition [4]. Notably, in primary cultures from from postnatal day 11 trigeminal ganglia tissue (containing a mix of trigeminal ganglion neurons and satellite glial cells) of FHM1 mutant mice, satellite glial cells exhibit an increased release of inflammatory mediators and an up-regulation of specific pro-algogenic receptors [5], but it is questionable whether findings in cultured cells can be translated to the intact trigeminal ganglion as no such increases were observed in isolated trigeminal ganglia from mice that were 11-14 weeks old [6]. In addition, trigeminal infiltration of macrophages was observed, pointing to the development of neuroinflammation in the peripheral nervous system [7]. Hence, both abnormal neuronal and glial cell function, and likely their interaction, may contribute to FHM pathophysiology. To further examine the involvement of glial cell activation in FHM, we here investigated whether the FHM1 R192Q missense mutation promotes the development of a reactive glia phenotype in the central nervous system of naïve mutant mice.

Methods

Animals

Three- to 4-month-old male homozygous FHM1 R192Q knock-in (KI) ("R192Q") and wild-type ("WT") mice were used. The KI mice were generated by introducing the human FHM1 pathogenic R192Q missense mutation in the orthologous *Cacna1a* gene using a gene targeting approach [8]. Genotyping was performed as described before [8]. Mice were kept under standard conditions (temperature: 22 ± 2°C; relative humidity: 50 ± 10%; light regimen: 12-hour light/12-hour dark cycle) with food and water *ad libitum*. All experimental procedures were in strict accordance with the Italian and EU regulation on animal welfare and were previously approved by the local ethics committee, and by the Italian Ministry of Health (authorization #736/2015-PR). All results are reported according to Animal Research: Reporting of In Vivo Experiments (ARRIVE) guidelines. Researchers were blinded for genotype information, and animals were randomised. Seven animals for both the WT and the FHM1 mutant group were analyzed per type of staining.

Immunohistochemistry

Mice were anesthetized with 1.5% isoflurane and perfused with 4% paraformaldehyde, as described [9]. Brains were removed, postfixed in 4% formalin for 60 minutes, cryoprotected in 30% sucrose for 24 hours, embedded in mounting medium (OCT; Tissue Tek, Sakura Finetek, Zoeterwoude, The Netherlands), and kept at -80°C until use. Twenty μm-thick coronal brain sections were collected for immunohistochemistry. Rabbit antibodies directed against: (i) astrocyte marker glial fibrillary acidic protein (anti-GFAP, 1:600; Dako, Milan, Italy), (ii) microglia marker ionized calcium binding adaptor molecule 1 (anti-Iba1, 1:500; Wako, Richmond, VA, USA), (iii) GPR17 receptor (home-made, 1:20,000); or mouse antibodies directed against mature oligodendrocyte marker glutathione S-transferase pi (anti-GSTπ, 1:500; MBL International, Woburn, MA, USA) were used. As secondary antibody, goat anti-rabbit or goat anti-mouse (1:600; Thermo Fisher Scientific, Monza, Italy)

conjugated to AlexaFluor®488 or AlexaFluor®555, respectively, were used. Cell nuclei were counterstained with the Hoechst33258 dye (1:20,000; Sigma-Aldrich, Milan, Italy). Cell staining was evaluated by a Zeiss Axioskop fluorescent microscope (Carl Zeiss, Milan, Italy), with the aid of the NIH ImageJ software, as described below.

Image analysis

Cell counting

For Iba1, GPR17, and GSTπ staining, the number of immunopositive cells was counted in whole sections and in selected brain areas (i.e., the cortex and corpus striatum) acquired at 20X magnification, and expressed as the number of cells/area in μm^2.

Densitometric analysis

For GFAP staining, a digital image of the immunostained brain sections was acquired at low (10X) magnification, and the mean values of pixel intensity were automatically evaluated by using the NIH Image-J software [10], and expressed as integrated density compared to values obtained in WT mice set to 100%.

Evaluation of microglia morphology and branch complexity

Fluorescent images of Iba1-positive microglia in the cortex and the corpus striatum were acquired at higher (40X) magnification, and converted to binary grayscale to better analyze cell morphology by the "Simple neurite tracer" tool of the Fiji-ImageJ software [11]. In each brain area, 3 randomly chosen cells in each of 10 randomly chosen optical fields (for a total of 30 cells/animal) were manually traced (see Figure 2A for representative images) and (i) the area covered by cell processes (which is proportional to the total cell ramification), (ii) the number of junctions and branches and the mean and maximal length of the latter (which reflects the complexity and ramification of cells),

and (iii) the number of triple and quadruple points (an additional indicator of cell complexity which indicates junctions where a single branch ramifies in three or four) were evaluated with the Skeleton analysis tool of the same software [11].

Western blotting

Western blotting analysis of brain tissues was performed, as described before [12]. Mouse antibodies directed against: i) GFAP (1:1,000; Cell Signaling, Danvers, MA, USA), or (ii) the marker of mature oligodendrocyte 2',3'-cyclic-nucleotide 3'-phosphodiesterase (CNPase, 1:250; Millipore, Vimodrone, MI, Italy) and rat antibody against myelin basic protein (MBP, 1:500; Millipore) as marker of myelinating oligodendrocytes, were used. Beta-actin (rabbit anti-β-actin, 1:1,500; Sigma-Aldrich) or α-tubulin (mouse anti α-tubulin, 1:1,000; Sigma-Aldrich) expression was analyzed as internal loading controls. Next, filters were incubated with species-specific secondary antibodies conjugated to horseradish peroxidase (goat anti-rabbit, 1:4,000 and goat anti-mouse, 1:2,000; both from Sigma-Aldrich; goat anti-rat, 1:2,000; Thermo Fisher Scientific). Protein detection was performed by ECL (BioRad, Milan, Italy). After autoradiography, the relative amount of protein was evaluated by the NIH Image-J software, normalized for the corresponding β-actin or α-tubulin values, and expressed with respect to values obtained in WT mice set to 1.

Statistical analysis

Scatter plots show single data and their mean±standard deviation (S.D.). Continuous variables were compared by use of Mann-Whitney *U* test. Two-tailed P-value<0.05 was considered statistically significant. Testing of hypotheses was performed by the free software R [13].

Results

Activated astrocytes in the naïve FHM1 R192Q mutant brain.

We first examined the expression of GFAP, a typical astrocyte marker whose expression is increased during reactive astrogliosis [14]. Counting cell number was not feasible, due to the complex interconnesions among cells; thus, we measured the fluorescence intensity of immunostaining (see Methods). In the WT cortex the highest abundance of stained cells is seen in the subventricular zone lining lateral ventricles (Figure 1A), similar to what was reported before for that brain region [15]. In the naïve FHM1 mutant mouse brain, however, GFAP immunoreactivity was typically present in higher cortical layers (Figure 1A; see magnification in inset), with a significant 19.3 ± 4.9% increase in fluorescence when compared to the WT brain (Figure 1B), suggesting reactive astrogliosis. Western blotting analysis of cortical tissue confirmed the results by showing a significant 25.4 ± 8.7% increase in GFAP expression. In the striatum, GFAP expression was not significantly increased (+26.3 ± 15.3%, P=0.32; Figure 1C), although the results were quite variable among samples. Moreover, Western blotting analysis of TG tissue also did not show a genotypic difference (normalized GFAP expression 1.00 ± 0.12 vs 1.19 ± 0.10 in the TG from WT and R192Q mice, respectively; P=0.144 Student's t test).

Hyper-ramified resident microglia in the naïve FHM1 R192Q mutant brain.

Next, we evaluated the number and morphology of microglial cells in the brains of FHM1 mutant and WT mice, to assess whether cells are in a resting, activated, or intermediate state [16]. The total number of Iba1-positive microglia cells in coronal brain sections was found significantly increased in FHM1 mutant mice (Figure 2A, 2B) suggesting cell proliferation. In both the cortex and corpus striatum, the increased cell number was paralleled by an increase in the total area covered by microglia ramifications (Figure 3A, C), as further evidenced by a higher number of long branches (Figure 3B-D), and of junctions and triple points which are representative of more complex ramification of cell processes (Figure 3E, F; see images in Figure 2A). The number of quadruple points was not different between the two groups (P=0.165; Figure 3G). Thus, our data show morphological changes of microglia towards a hyperramified intermediate state [16], which likely

reflects cell adaptation in response to changes in the (pathological) environment [16], and suggest an intensification of surveillance of this cell population.

No basal changes in markers of mature oligodendrocytes in the FHM1 mutant brain.

Based on the known reciprocal influence of neurons and oligodendrocytes, we have also evaluated possible changes in the expression of markers of myelination in the brains of FHM1 mutant mice. Counting the number of CNPase-positive mature and MBP-positive myelinating oligodendrocytes after immunohistochemistry [17] was not possible due to the high number of cells with a very complex morphology (not shown). We, therefore, performed semi-quantitative Western blotting analysis of portions of the cortex from naïve FHM1 R192Q and WT mice. Results show no alteration in the expression of either protein (CNPase: cortex, P=0.295; c. striatum, P=0.836; MBP: cortex, P=0.945; c. striatum, P=0.445; Figure 4). Nevertheless, a reduction in the number of immature and pre-oligodendrocytes expressing the GPR17 receptor [18] was detected in FHM1 mutant brains (P=0.017; Figure 5A, B). When analyzing specific brain areas, differences in the number of GPR17-expressing cells were observed in the corpus striatum (P=0.038), with similar values (P=0.465) in the cortex (Figure 5B), whereas the expression of GSTπ, a marker of intermediate oligodendrocyte maturation was similar between WT and FHM1 mice (65.6 ± 25.6 vs. 59.4 ± 17.6 positive cells/counted field, respectively; P=0.390). Overall, our results suggest that the activity of mutated neuronal $Ca_V2.1$ channels does not alter the basal maturation of oligodendrocytes but reduces the fraction of immature and pre-oligodendrocytes expressing GPR17.

Discussion

Here we present evidence for increased glial cell reactivity in the naïve FHM1 R192Q mouse brain, as evidenced bymorphological signs of astrogliosis, and of reactive microglia. Because of the previously reported increased glutamate neurotransmitter release from excitatory cortical neurons in

the FHM1 mutant brain [3], we set out to investigate whether the observed enhanced neurotransmission could also modify neuron-to-glia cell communication, directly or indirectly, and promote the basal activation of resident glial cells, thus contributing to the FHM1 phenotype.

Given that non-neuronal cells, in particular glia cells, contribute to the initiation and maintenance of chronic pain [19], which is now referred to as a "gliopathy" [20], one possible role of permanently activated astrocytes and microglia is to contribute to the pathological brain environment relevant to FHM1 pathology.

Both astrocytes and microglia can respond to external stimuli and to changes in the environment by exerting either detrimental or protective functions [14, 16]. Although we do not have functional evidence of the polarization of these cells towards an overall pro- or anti-inflammatory phenotype in FHM1 brain, it is relevant that here we detected changes in cell morphology, which for glial cells represent an indicative parameter of altered cell function, in the absence of a CSD trigger. Our data show that the presence of mutant neuronal $Ca_V2.1$ channels leads to what we would interpret as an adaptation of glial cells that have to cope, from time to time, with increased levels of glutamate (and likely ATP) and K^+ ions, and likely prime cells to be ready to react to possible subsequent triggers.

Concerning astrocytes, consistent with the known role of calcium waves in cell-to-cell communication [21], here we have detected signs of reactive astrogliosis and we can speculate that this could be a factor that modulates headache pain. Afterall, astrocytes play a key role in the blood-brain barrier and control of the blood-brain exchanges of chemicals and other potential migraine triggers, such as certain nutrients [14]. Additionally, glial cell dysfunction has been implicated in FHM2 mutant mice [22. 23], in which loss-of-function mutations in the $\alpha2$ subunit of Na^+/K^+ ATPases expressed in astrocytes resulted in increased cortical glutamatergic neurotransmission, but in this case as the result of inadequate K^+ and glutamate buffering ability due to abnormal glial function [24]. Similar to FHM1 mice, FHM2 mice were shown to be more susceptible to experimentally induced CSD [22, 25]. Thus, data from a different model of FHM suggests that astrocytes can contribute to migraine pathology.

Microglia are the immunocompetent cells in the central nervous system, which constantly scan the environment and contact surrounding neurons and astrocytes. Under pathological conditions, microglia acquire an activated phenotype, accompanied by the release of cytokines, increased proliferation, migration and phagocytic activity [19]. Increased neuronal activity, as seen in epilepsy or during CSD propagation [26, 27], is another trigger for microglia reaction. Additionally, higher microglia dynamic movements are detected hours after induction of CSD, and the level of microglia activation is proportional to the number of CSD waves [28]. The transition between resting and fully activated (i.e., amoeboid phagocytic microglia) is characterized by the presence of an intermediate phenotype, which can be recognized by increased branching as in naïve FHM1 brain, representing a "warning" state of cells to be fully able to respond to subsequent harms [16]. Very recent data show that elongation of processes is mandatory for microglia to shift from a pro- to an anti-inflammatory phenotype, which can more efficiently patrol the surrounding brain tissue [29]. Thus, simply based on changes in cell morphology we cannot definitively assume whether hyper-ramified microglia have an overall detrimental or beneficial role. Further studies are needed to analyze the expression of specific markers of microglia polarization towards anti-inflammatory M1 or pro-inflammatory M2 phenotype [16]. Nevertheless, we can conclude that in FHM1 mutant brains under basal conditions, already after minor disturbances in brain activity, microglia enlarge their area of patrolling by extending cell processes being therefore able to react more efficiently, if needed, and to release various signaling molecules involved in the cross-talk with the other cell populations.

Oligodendrocytes and their precursor cells (OPCs) are also involved in cell-to-cell communication in the brain by reacting to neuronal signals and to activated astrocytes and surrounding microglial cells [30, 31]. To confirm their relevance to migraine pathology, altered patterns of myelination have been observed in the brains of migraineurs [32], and transient disruption of myelin structure is induced by CSD [33]. Our data show no basal changes in the expression of mature oligodendrocytes in FHM1 brains, but a significant reduction of GPR17 expression.

As GPR17 receptor expression must be down-regulated to allow for the terminal maturation of pre-oligodendrocytes [34], its reduced expression could accelerate oligodendrocyte maturation. Nevertheless, since GPR17-expressing OPCs show a higher susceptibility to toxic signals, such as pathologically elevated concentrations of ATP [18] that are likely to be found in the FHM1 mutant brain as an additional consequence of the enhanced glutamatergic transmission [35], at present we cannot exclude that the observed reduction in their number is due to cell death.

A recent genetic study, which used genotype data from thousands of migraine patients and controls tested in genome-wide association studies (GWAS), evaluated gene sets containing astrocyte- and oligodendrocyte-related genes and found an association with the common forms of migraine [36]. This supports the concept that genetic factors underlie glial cell dysfunction in migraine, so beyond the correlation presented here in FHM1 mutant mice. Glia cell activation, which is suggestive of neuroinflammation, may therefore be relevant to various types of migraine, although this has not firmly been established for common forms of migraine. It might be that glial cell activation is a relevant reflection of the basal reactive state of a FHM1 mutant brain that might influence how migraine triggers affect the brain. In that respect it is of interest that experimentally induced CSDs generate a molecular signature of activated inflammatory pathways specifically linked to interferon-γ signaling that is seen in the FHM1 mutant mice, but not the wild-type control mice [37]. Together with data in FHM2 mice (see above), all in all the information supports the involvement of glial dysfuctions eventually leading to neuroinflammation in a migraine-relevant context.

As mentioned above, one limitation of our study is that the claim of glial cell activation in FHM1 mutant brains is only based on changes in cell morphology, i.e., without investigating its functional consequences. Still, the observed features are regarded as highly representative of the functional state of the cells, so can be considered sufficient proof that our findings are genuine.

Taken together, we provided evidence that FHM1 mutations, at least the R192Q missense mutation, in a transgenic mouse model, not only impacts neurons, but also glia cells. This study therefore reinforces the concept that altered neuron-to-glia communication in naïve FHM1 mutant mice might

contribute to the disease phenotype, and that normalizing glia cell function could have potential to treat migraine. We feel that our observations are relevant to the understanding of (hemiplegic) migraine pathophysiology as one could ask the question whether the same occurs in patients.

Funding

This work has been partially supported by the Fondazione Cariplo (Grant #2011-0505 to MPA), by the Department of Excellence grant program from the Italian Ministry of Research (MIUR), the Center of Medical System Biology (CMSB) established by the Netherlands Genomics Initiative/Netherlands Organisation for Scientific Research (NGI/NWO) (to AMJMvdM), and the European Community (EC) FP7-EUROHEADPAIN (no. 602633 to AMJMvdM).

Key Findings

- Reactive astrocytes and activated microglia in the brains of FHM1 mutant mice that express neuronal $Ca_V2.1$ calcium channels with R192Q-mutated α_{1A} subunits under basal conditions
- Normalization of glia cell reactivity maybe a promising avenue for drug treatment

References

1. Headache Classification Committee of the International Headache Society (IHS). The International Classification of Headache Disorders, 3rd edition (beta version). *Cephalalgia* 2013; 33: 629-808.
2. Tottene A, Conti R, Fabbro A, et al. Enhanced excitatory transmission at cortical synapses as the basis for facilitated spreading depression in Ca(v)2.1 knockin migraine mice. *Neuron* 2009; 61: 762-773.
3. Ferrari MD, Klever RR, Terwindt GM, et al. Migraine pathophysiology: lessons from mouse models and human genetics. *Lancet Neurol* 2015; 14: 65-80.
4. Xanthos DN, Sandkühler J. Neurogenic neuroinflammation: inflammatory CNS reactions in response to neuronal activity. *Nat Rev Neurosci* 2014; 15: 43-53.
5. Ceruti S, Villa G, Fumagalli M, et al. Calcitonin gene-related peptide-mediated enhancement of purinergic neuron/glia communication by the algogenic factor bradykinin in mouse trigeminal ganglia from wild-type and R192Q Cav2.1 Knock-in mice: implications for basic mechanisms of migraine pain. *J Neurosci* 2011; 31: 3638-3649.
6. Chan KY, Labastida-Ramírez A, Ramírez-Rosas MB, et al. Trigeminovascular calcitonin gene-related peptide function in Cacna1a R192Q-mutated knock-in mice. *J Cereb Blood Flow Metab* 2019; 39: 718-729.
7. Franceschini A, Vilotti S, Ferrari MD, et al. TNFα levels and macrophages expression reflect an inflammatory potential of trigeminal ganglia in a mouse model of familial hemiplegic migraine. *PLoS One.* 2013; 8: e52394.
8. van den Maagdenberg AM, Pietrobon D, Pizzorusso T, et al. A Cacna1a knockin migraine mouse model with increased susceptibility to cortical spreading depression. *Neuron* 2004; 41: 701-710.

9. Villa G, Ceruti S, Zanardelli M, et al. Temporomandibular joint inflammation activates glial and immune cells in both the trigeminal ganglia and in the spinal trigeminal nucleus. *Mol Pain* 2010; 6: 89.

10. Schneider CA, Rasband WS, Eliceiri KW NIH Image to ImageJ: 25 years of image analysis. *Nature Methods* 2012; 9: 671-675.

11. Schindelin J, Arganda-Carreras I, Frise E et al. Fiji: an open-source platform for biological-image analysis. *Nat Meth* 2012; 9: 676-682.

12. Magni G, Merli D, Verderio C, et al. $P2Y_2$ receptor antagonists as anti-allodynic agents in acute and sub-chronic trigeminal sensitization: role of satellite glial cells. *Glia* 2015; 63: 1256-1269.

13. R Development Core Team. R: A language and environment for statistical computing. *R Foundation for Statistical Computing.* Vienna, Austria. https://www.R-project.org/ (2016, accessed 15 February 2019).

14. Buffo A, Rolando C, Ceruti S. Astrocytes in the damaged brain: molecular and cellular insights into their reactive response and healing potential. *Biochem Pharmacol* 2010; 79: 77-89.

15. Boccazzi M, Rolando C, Abbracchio MP, et al. Purines regulate adult brain subventricular zone cell functions: contribution of reactive astrocytes. *Glia* 2014; 62: 428-439.

16. Walker FR, Beynon SB, Jones KA, et al. Dynamic structural remodelling of microglia in health and disease: a review of the models, the signals and the mechanisms. *Brain Behav Immun* 2014; 37: 1-14.

17. Barateiro A and Fernandes A. Temporal oligodendrocyte lineage progression: in vitro models of proliferation, differentiation and myelination. *Biochim Biophys Acta* 2014; 1843: 1917-1929.

18. Ceruti S, Viganò F, Boda E, et al. Expression of the new P2Y-like receptor GPR17 during oligodendrocyte precursor cell maturation regulates sensitivity to ATP-induced death. *Glia* 2011; 59: 363-378.

19. Salter MW and Stevens B. Microglia emerge as central players in brain disease. *Nat Med* 2017 23: 1018-1027.

20. Ji RR, Berta T, Nedergaard M. Glia and pain: is chronic pain a gliopathy? *Pain* 2013; 154 Suppl 1: S10-S28.

21. de Bock M, Decrock E, Wang N, et al. The dual face of connexin-based astroglial Ca(2+) communication: a key player in brain physiology and a prime target in pathology. *Biochem Biophys Acta* 2014; 1843: 2211-2232.

22. Leo L, Gherardini L, Barone V, et al. Increased susceptibility to cortical spreading depression in the mouse model of familial hemiplegic migraine type 2. *PLoS Genet* 2011; 7(6): e1002129.

23. Bøttger P, Glerup S, Gesslein B, et al. Glutamate-system defects behind psychiatric manifestations in a familial hemiplegic migraine type 2 disease-mutation mouse model. *Sci Rep* 2016; 6: 22047.

24. Capuani C, Melone M, Tottene A, et al. Defective glutamate and K+ clearance by cortical astrocytes in familial hemiplegic migraine type 2. EMBO Mol Med 2016; 8: 967-986.

25. Kros L, Lykke-Hartmann K, Khodakhah K. Increased susceptibility to cortical spreading depression and epileptiform activity in a mouse model for FHM2. *Sci Rep* 2018; 8: 16959.

26. Wendt S, Wogram E, Korvers L, Kettenmann H. Experimental Cortical Spreading Depression Induces NMDA Receptor Dependent Potassium Currents in Microglia. *J Neurosci* 2016; 36: 6165-6174.

27. Grinberg YY, Milton JG, Kraig RP. Spreading Depression Sends Microglia on Lévy Flights. *PLoSOne* 2011; 6: e19294.

28. Shibata M and Suzuki N. Exploring the role of microglia in cortical spreading depression in neurological disease. *J Cereb Blood Flow Metab* 2017; 37: 1182-1191.

29. Yang R, Wang H, Wen J, et al. Regulation of microglial process elongation, a featured characteristic of microglial plasticity. *Pharmacol Res* 2019; 139: 286-297.
30. Maldonado PP and Angulo MC. Multiple Modes of Communication between Neurons and Oligodendrocyte Precursor Cells. *Neuroscientist* 2015; 21: 266-276.
31. Lundgaard I, Osório MJ, Kress BT, et al. White matter astrocytes in health and disease. *Neuroscience* 2014; 276: 161-173.
32. Granziera C, Daducci A, Romascano D, et al. Structural abnormalities in the thalamus of migraineurs with aura: a multiparametric study at 3 T. *Hum Brain Mapp* 2014; 35: 1461-1468.
33. Pusic AD, Mitchell HM, Kunkler PE, et al. Spreading depression transiently disrupts myelin via interferon-gamma signaling. *Exp Neurol* 2015; 264: 43-54.
34. Fumagalli M, Daniele S, Lecca D, et al. Phenotypic changes, signaling pathway, and functional correlates of GPR17-expressing neural precursor cells during oligodendrocyte differentiation. *J Biol Chem* 2011; 286: 10593-10604.
35. Burnstock G. Purinergic cotransmission. *Exp Physiol* 2009; 94: 20-24.
36. Eising E, de Leeuw C, Min JL, et al. Involvement of astrocyte and oligodendrocyte gene sets in migraine. *Cephalalgia* 2016; 36: 640-647.
37. Eising E, Shyti R, 't Hoen PAC, et al. Cortical Spreading Depression Causes Unique Dysregulation of Inflammatory Pathways in a Transgenic Mouse Model of Migraine. *Mol Neurobiol* 2017; 54: 2986-2996.

Figure legends

Figure 1. Reactive astrogliosis in the naïve FHM1 mutant mouse brain. A: coronal sections from the brains of wild-type (WT) and R192Q mutant mice stained with anti-GFAP antibody. Representative pictures are shown with magnified details. Scale bars: 1.5 mm. B: quantification of GFAP immunoreactivity by densitometric analysis. Scatter plots show the results obtained in seven animals for each group. The pixel intensity values are expressed as mean ± S.D. compared to WT animals set to 100%. P=0.007 with respect to WT, two-tailed non-parametric Mann-Whitney test. C: evaluation of GFAP expression in cortical and striatal tissue by Western blotting. β-actin was utilized as internal loading control (see representative filters at the bottom). Scatter plots show the optical density of protein bands from seven animals for each group normalized on corresponding β-actin and expressed as mean ± S.D. with respect to WT animals set to 1. P=0.028 (cortex) and P=0.32 (c. striatum) with respect to WT, two-tailed non-parametric Mann-Whitney test.

Figure 2. Increased number of microglia in the naïve FHM mutant brain. A: Representative pictures of coronal sections from the brains of wild-type (WT) and R192Q mutant mice stained with primary antibody against Iba1 (40X magnification; scale bars: 25 μM). Magnified details show representative cells traced with the «Simple neurite tracer» tool of the Fiji-ImageJ software. Junctions and branches are indicated. B: the total number of Iba1-positive microglial cells was counted in brain sections (20X magnification; not shown). Scatter plots show the mean ± S.D. of Iba1-positive cell number/area from seven animals for each group. P=0.002 with respect to WT, two-tailed non-parametric Mann-Whitney test.

Figure 3. Increased branching and complexity of microglia in the cortex and corpus striatum of FHM1 mutant mice. The complexity and ramification of Iba1-positive cells was evaluated by the Skeleton analysis tool of the Fiji-ImageJ software (see Methods section). In both cortex and c. striatum from wild-type (WT) and R192Q mutant mice, scatter plotsshow: (A) the area covered by

the cell projection tree; (B) the total number, (C) the average and (D) the maximal length of branches; (E) the total number of junctions and of (F) triple and (G) quadruple points. Data are the mean ± S.D. of 30 randomly chosen cells/animal from seven animals for each group (see Methods for details). (A) P=0.0006 (cortex and c. striatum); (B) P=0.004 (cortex) and P=0.038 (c. striatum); (C) P=0.053 (cortex) and P=0.026 (c. striatum); (D) P=0.007 (cortex) and P=0.004 (c. striatum); (E) P=0.011 (cortex and c. striatum); (F) P=0.011 (cortex) and P=0.038 (c. striatum); (G) P=0.165 (cortex and c. striatum), two-tailed non-parametric Mann-Whitney test.

Figure 4. No changes in the expression of markers of mature oligodendrocytes in the brains of FHM1 mutant mice. A: Western blotting evaluation of CNPase and MBP expression in cortical and striatal tissues from wild-type (WT) and R192Q mutant mice. Alpha-tubulin was utilized as internal control for protein loading (see representative filters of cortex samples in B). The three MBP bands at different molecular weights (some 15-16-18 kDa) were analyzed together. Scatter plots show the optical density of protein bands from seven animals for each group expressed as mean ± S.D. with respect to WT animals set to 1. In (A) CNPase: P=0.295 (cortex) and P=0.836 (c. striatum); MBP: P=0.945 (cortex) and P=0.445 (c. striatum), two-tailed non-parametric Mann-Whitney test.

Figure 5: Reduced number of GPR17-positive cells in the FHM mutant brain. A: representative pictures of coronal sections from the brains of wild-type (WT) and R192Q mutant mice stained with an home-made antibody against the membrane receptor GPR17. Cell nuclei were counterstained with the Hoechst33258 dye. The number of GPR17-positive cells was counted in the entire coronal section and in selected brain areas, i.e., the cortex and the corpus striatum. Scale bars: 1.5 mm. B: scatter plots show the mean ± S.D. of GPR17-positive cell number/counted field in the different brain areas. Data were obtained by counting ten sections from seven independent animals/group. *P=0.017 (total

number of cells), P=0.456 (*cortex*) and P=0.038 (*c.* striatum) with respect to WT, two-tailed non-parametric Mann-Whitney test.

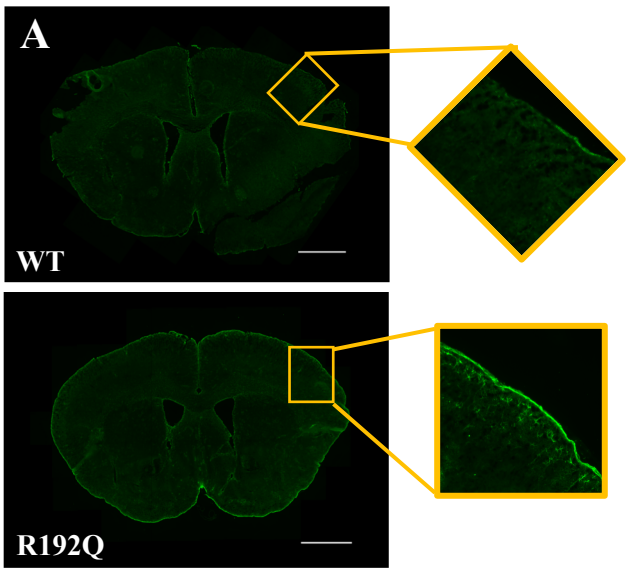
A
WT
R192Q

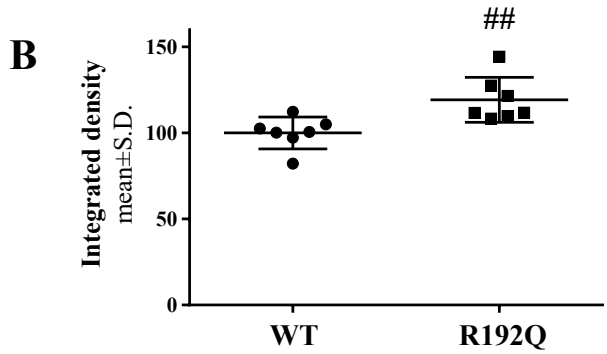
B
Integrated density
mean±S.D.
150
100
50
0
##
WT
R192Q

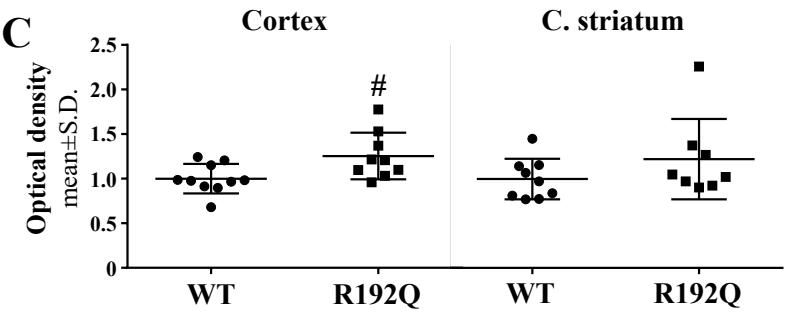
C
Cortex
C. striatum
Optical density
mean±S.D.
2.5
2.0
1.5
1.0
0.5
0
#
WT
R192Q
WT
R192Q

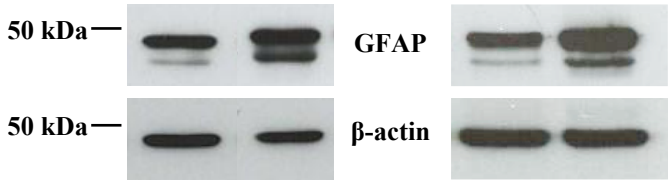
50 kDa
GFAP
50 kDa
β-actin

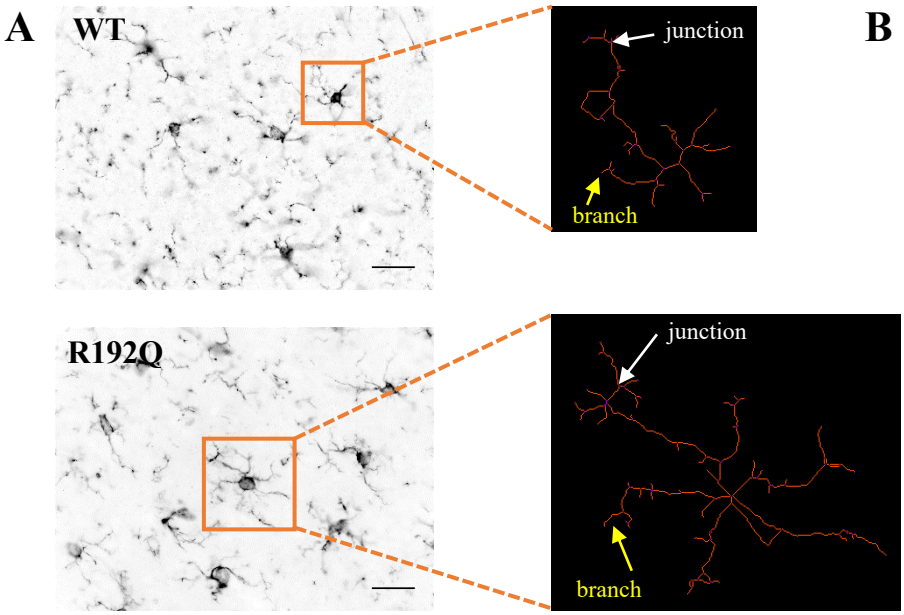
A
WT
junction
branch
R192Q
junction
branch

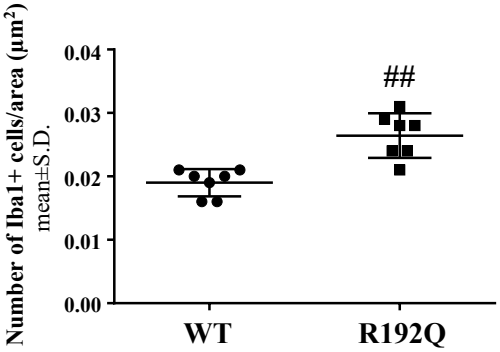
B
Number of Iba1+ cells/area (μm²)
mean±S.D.
0.04
0.03
0.02
0.01
0.00
##
WT
R192Q

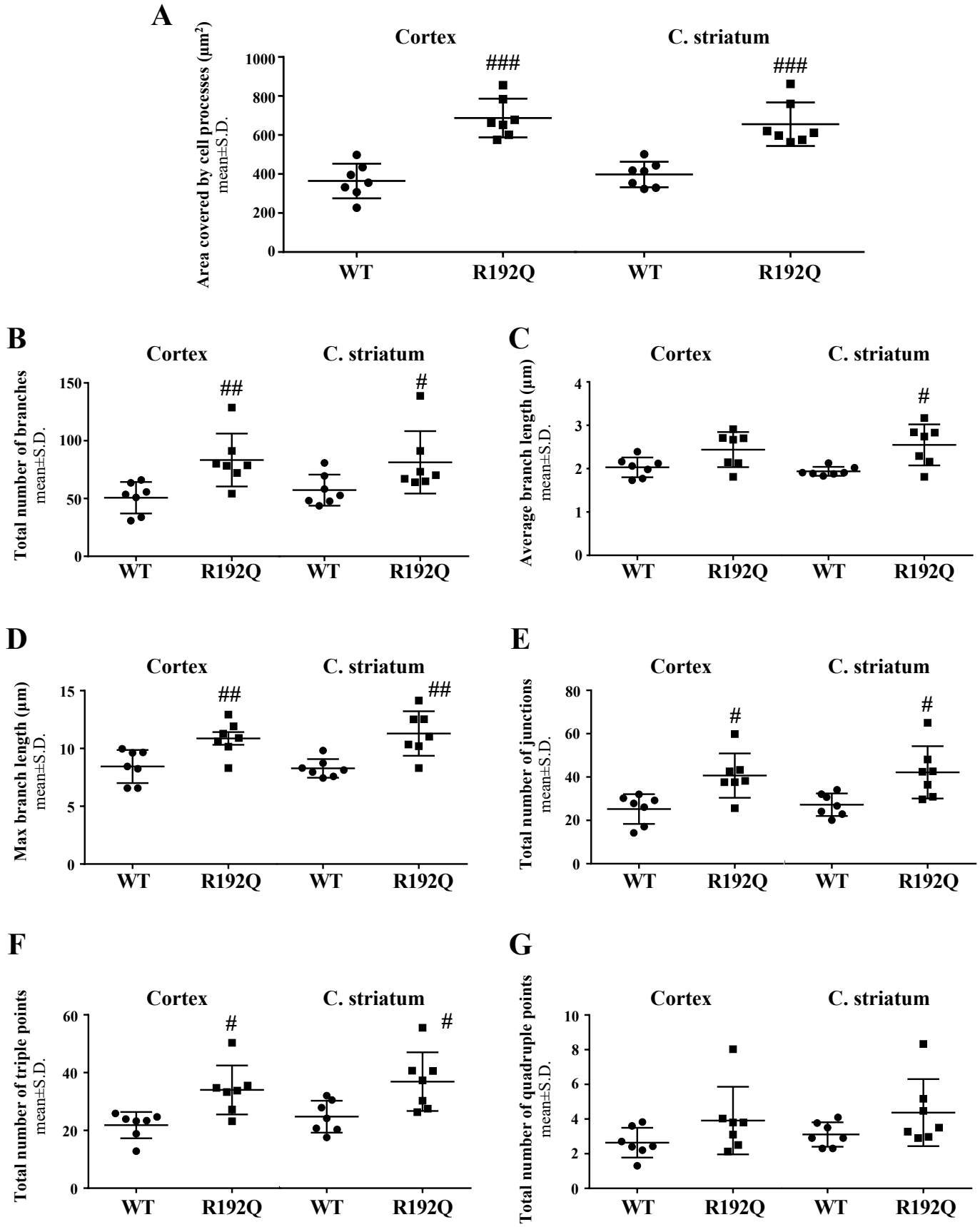
A
Cortex
C. striatum
Area covered by cell processes (µm²)
mean±S.D.
1000
800
600
400
200
0
###
###
WT
R192Q
WT
R192Q
B
Cortex
C. striatum
Total number of branches
mean±S.D.
150
100
50
0
##
#
WT
R192Q
WT
R192Q
C
Cortex
C. striatum
Average branch length (µm)
mean±S.D.
4
3
2
1
0
#
WT
R192Q
WT
R192Q
D
Cortex
C. striatum
Max branch length (µm)
mean±S.D.
15
10
5
0
##
##
WT
R192Q
WT
R192Q
E
Cortex
C. striatum
Total number of junctions
mean±S.D.
80
60
40
20
0
#
#
WT
R192Q
WT
R192Q
F
Cortex
C. striatum
Total number of triple points
mean±S.D.
60
40
20
0
#
#
WT
R192Q
WT
R192Q
G
Cortex
C. striatum
Total number of quadruple points
mean±S.D.
10
8
6
4
2
0
WT
R192Q
WT
R192Q

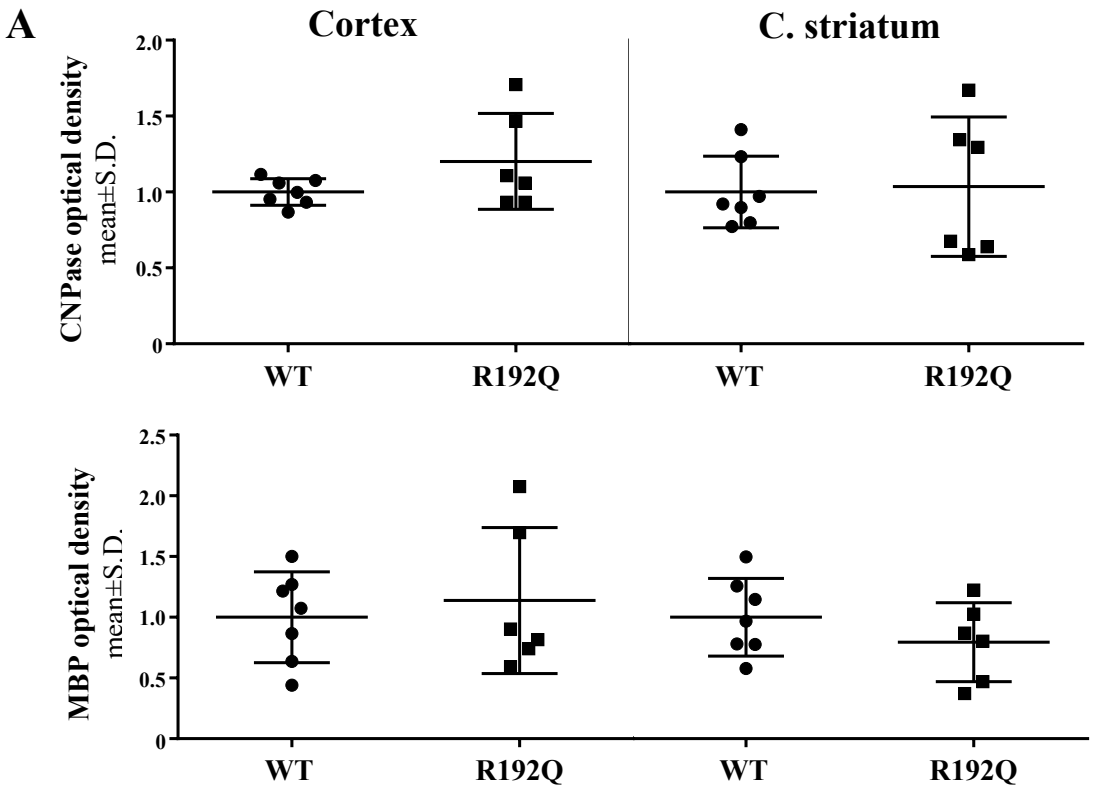
A
Cortex
C. striatum
CNPase optical density
mean±S.D.
2.0
1.5
1.0
0.5
0
WT
R192Q
WT
R192Q
MBP optical density
mean±S.D.
2.5
2.0
1.5
1.0
0.5
0
WT
R192Q
WT
R192Q

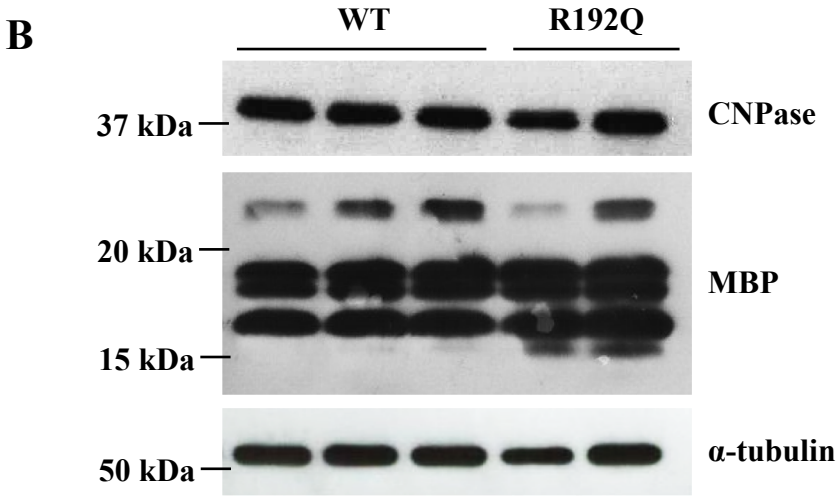
B
WT
R192Q
37 kDa
CNPase
20 kDa
MBP
15 kDa
50 kDa
α-tubulin

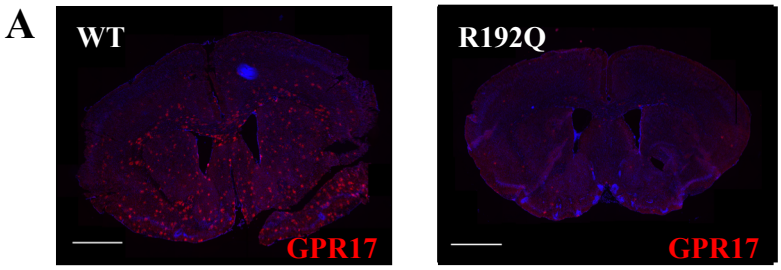
A
WT
GPR17
R192Q
GPR17

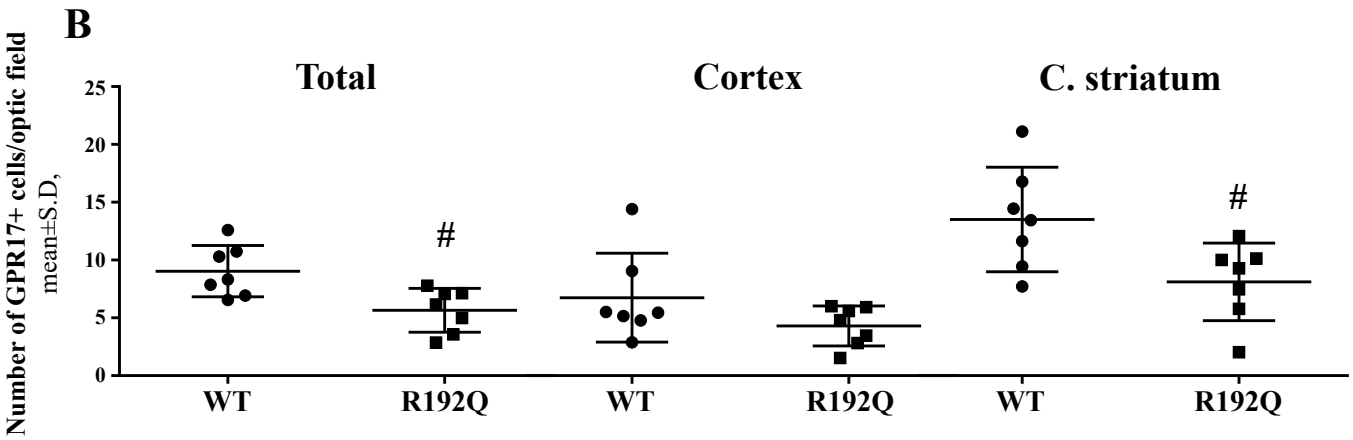
B
Total
Cortex
C. striatum
Number of GPR17+ cells/optic field
mean±S.D,
25
20
15
10
5
0
#
#
WT
R192Q
WT
R192Q
WT
R192Q